JOURNAL OF THERMOPHYSICS AND HEAT TRANSFER
Vol. 10, No. 3, July–September 1996

Laminar Natural Convection Flow over a Vertical Forward-Facing Step

H. I. Abu-Mulaweh,* B. F. Armaly,† and T. S. Chen‡
University of Missouri–Rolla, Rolla, Missouri 65409

Measurements and predictions of laminar boundary-layer flow in natural convection over a vertical forward-facing step are reported. Laser Doppler velocimeter and cold-wire anemometer are used to simultaneously measure the velocity and temperature distributions, respectively. Flow visualization is also performed to determine the reattachment lengths. The upstream and downstream walls and the step itself are heated to a uniform and constant temperature. The experiment is carried out for a range of step heights $8 \le s \le 16$ mm, temperature differences $6.5 \le \Delta T \le 23$°C between the heated wall and the freestream, and reference velocities $0.255 \le u^* \le 0.48$ m/s. These results reveal that the step height and the buoyancy force, induced by the temperature difference, significantly affect the velocity and temperature distributions and the rate of heat transfer from the heated wall. The measured results agree well with numerical predictions.

Nomenclature

C_f = friction coefficient, $\tau_w/(\rho u^{*2}/2)$
Gr_{xi} = Grashof number, $g\beta(T_w - T_0)x_i^3/\nu^2$
g = gravitational acceleration
H = height of computational domain
h = local heat transfer coefficient, $-k(\partial T/\partial y)_{y=0}/(T_w - T_\infty)$
k = thermal conductivity
Nu = local Nusselt number, hx_i/k
P = dimensionless pressure, $(p + \rho gx)/(\rho_\infty u^{*2})$
Pr = Prandtl number, ν/α
p = pressure
Re_{xi} = Reynolds number, $u^* x_i/\nu$
S = dimensionless step height, s/x_i
s = step height
T = fluid temperature
T_w = wall temperature
T_0 = inlet temperature
T_∞ = local freestream temperature
U = dimensionless streamwise velocity component, u/u^*
u = streamwise velocity component
u^* = reference velocity, $[g\beta(T_w - T_0)x_i]^{1/2}$
V = dimensionless transverse velocity component, v/u^*
v = transverse velocity component
X, Y = dimensionless streamwise and transverse coordinates, x/x_i, y/x_i
X_e, X_i, X_m, X_r, X^* = x_e/x_i, x_i/x_i, x_m/x_i, x_r/x_i, x^*/x_i
x, y = streamwise and transverse coordinates
x_e = downstream length behind the step
x_i = inlet length upstream of the step
x_m = location of maximum Nusselt number
x_r = reattachment length
x^* = $x + xi$
Y^* = $(y + s)/x_i$
α = thermal diffusivity
β = volumetric thermal expansion coefficient
ΔT = temperature difference, $(T_w - T_0)$
δ_s = boundary-layer thickness at the step
θ = dimensionless temperature, $(T - T_0)/(T_w - T_0)$
θ_∞ = $(T_\infty - T_0)/(T_w - T_0)$
ν = kinematic viscosity

Received July 19, 1995; revision received Jan. 8, 1996; accepted for publication Jan. 9, 1996.

*Lecturer in Mechanical Engineering, Department of Mechanical and Aerospace Engineering and Engineering Mechanics.

†Professor of Mechanical Engineering, Department of Mechanical and Aerospace Engineering and Engineering Mechanics. Member AIAA.

‡Curators' Professor of Mechanical Engineering, Department of Mechanical and Aerospace Engineering and Engineering Mechanics. Associate Fellow AIAA.

Introduction

FLOW separation and recirculation caused by a sudden compression in flow geometry, such as a forward-facing step, play an important role in the design of heat transfer devices, such as cooling systems for electronic equipment, high-performance heat exchangers, combustion chambers, cooling passages of turbine blades, and chemical process equipment. For the flow past a forward-facing step, one or two separated regions may develop, one upstream and the other downstream from the step, depending on the ratio of the boundary-layer thickness at the step to the step height, as reported by Abu-Mulaweh et al.[1] In the past, several investigators have dealt with the fluid flow and heat transfer characteristics over a two-dimensional forward-facing step (see e.g., Abu-Mulaweh et al.,[1-3] and Baron et al.[4] and the references cited therein). However, in these studies the attention was focused on the forced and mixed convection regimes. The flow over a two-dimensional rib will exhibit some of the general behavior of forward-facing step geometry. Natural convection flows in vertical channels with single or multiple heated ribs were investigated in Refs. 5–10. However, these investigations are qualitative in nature and do not provide sufficient details of the flow and thermal fields for the natural convection over a forward-facing step geometry. The lack of flow and heat transfer measurements in natural convection over a heated vertical forward-facing step geometry has motivated the present study.

In this study, consideration is given to buoyancy-induced natural convection laminar boundary-layer airflow over a two-dimensional, vertical forward-facing step. The upstream and downstream walls and the step itself are heated to a uniform and constant temperature, as shown schematically in Fig. 1.

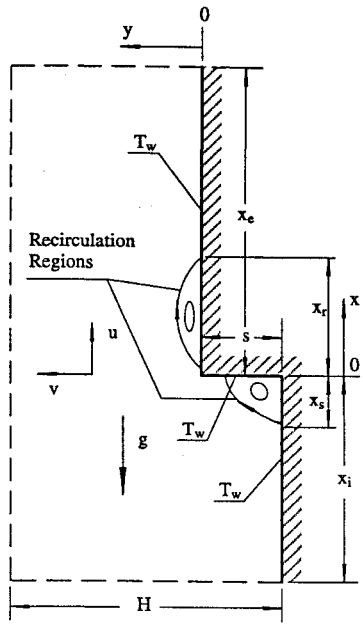

Fig. 1 Schematics diagram of the computation domain.

Results of interest, such as velocity and temperature distributions, reattachment lengths, and local heat transfer coefficients are reported to illustrate the effects of step height and buoyancy force on these parameters.

Experimental Apparatus and Procedure

The experimental study was performed in an existing low-turbulence, open-circuit air tunnel. Details of the air tunnel have been described by Ramachandran et al.[11] In this experiment, the forward-facing step geometry in the test section of the tunnel was identical to that used by Abu-Mulaweh et al.,[2] except that the wall upstream of the step was also heated and maintained at the same uniform temperature as the downstream wall. The forward-facing step geometry was formed by an upstream section (30.48 cm long), a step (8–16 mm), and a downstream section (79 cm long) behind the step. The test section (step geometry) spanned the entire width of the tunnel (30.48 cm). The entire heated step geometry was instrumented with thermocouples and with heaters that were individually controlled to maintain the surface at a uniform temperature, as described by Abu-Mulaweh et al.[12] This heating arrangement provided the capability of maintaining the entire heated plate at any desired uniform temperature to within 0.2°C. The airflow velocities and temperatures were measured by a laser Doppler velocimeter (LDV) and a cold-wire anemometer, respectively. The repeatability of the air velocity measurements was within 3%, and that of the air temperature measurements was within 0.05°C. Glycerin smoke particles, 2–5 μm in diameter, generated by immersing a 100-W heating element into a glycerin container, were mixed with the airflow to provide the scattering particles for LDV measurements and also for flow visualizations. The flow visualization, performed with the aid of a 15-W collimated white light beam, 2.5 cm in diameter, was used to probe the flow domain for measuring the reattachment length.

Numerical Analysis

The experimental geometry and boundary conditions were also modeled for numerical simulation, as shown schematically in Fig. 1. The lengths x_i, x_e, s, and H in the figure are not presented to the same scale. They are selected for clarity. The upstream and downstream walls and the step itself were considered as being heated to a uniform temperature T_w. The gravitational acceleration was acting vertically downward, and the calculation domain had a length of $x_i + x_e$ and a height of H, which was selected to be 10 cm.

In the analysis, the fluid properties were considered to be constant and evaluated at T_0. By utilizing the Boussinesq approximation ($\beta\Delta T < 0.1$ in this experiment), the governing conservation equations for the physical problem under consideration can be written in nondimensional form as follows:

Continuity:

$$\frac{\partial U}{\partial X} + \frac{\partial V}{\partial Y} = 0 \tag{1}$$

X momentum:

$$\frac{U\partial U}{\partial X} + \frac{V\partial U}{\partial Y} = \frac{-\partial P}{\partial X} + Gr_{xi}^{-1/2}\left(\frac{\partial^2 U}{\partial X^2} + \frac{\partial^2 U}{\partial Y^2}\right) + (\theta - \theta_\infty) \tag{2}$$

Y momentum:

$$\frac{U\partial V}{\partial X} + \frac{V\partial V}{\partial Y} = \frac{-\partial P}{\partial Y} + Gr_{xi}^{-1/2}\left(\frac{\partial^2 V}{\partial X^2} + \frac{\partial^2 V}{\partial Y^2}\right) \tag{3}$$

Energy:

$$\frac{U\partial\theta}{\partial X} + \frac{V\partial\theta}{\partial Y} = (Pr^{-1}Gr_{xi}^{-1/2})\left(\frac{\partial^2\theta}{\partial X^2} + \frac{\partial^2\theta}{\partial Y^2}\right) \tag{4}$$

The boundary conditions for the previous set of governing equations are as follows:

Upstream inlet conditions at $X = -1$:

$$U = 0, \qquad \frac{\partial V}{\partial X} = 0, \qquad \theta = 0 \tag{5}$$

Downstream exit conditions at $X = X_e$:

$$\frac{\partial U}{\partial X} = 0, \qquad \frac{\partial V}{\partial X} = 0, \qquad \frac{\partial\theta}{\partial X} = 0 \tag{6}$$

Freestream boundary at $Y = (H/x_i) - S$ and $-1 \le X \le X_e$:

$$U = 0, \qquad \frac{\partial V}{\partial Y} = 0, \qquad \theta = \theta_\infty \tag{7}$$

Stepped wall: 1) upstream of the step at $Y = -S$ and $-1 \le X \le 0$,

$$U = 0, \qquad V = 0, \qquad \theta = 1 \tag{8}$$

2) at the step $X = 0$ and $-S \le Y \le 0$,

$$U = 0, \qquad V = 0, \qquad \theta = 1 \tag{9}$$

and 3) downstream of the step at $Y = 0$ and $0 \le X \le X_e$:

$$U = 0, \qquad V = 0, \qquad \theta = 1 \tag{10}$$

The numerically stated boundary conditions simulate, as closely as possible, the conditions in this experiment.

The SIMPLE algorithm as described by Patankar[13] was utilized to obtain the solution of the coupled partial differential equations. The initial velocity and pressure distributions inside the flow domain were set to zero and the initial temperature distribution was set as uniform and equal to the inlet fluid temperature. Since the buoyancy force term appears in the momentum equation, the thermal field and the flowfield are coupled, and they have to be solved simultaneously. The momentum equations were solved first based on the temperature and the velocity values from the previous iteration step, and then the energy equation was solved to update the temperature field.

This process was repeated for each iteration step until a converged solution was obtained.

In this study, the upstream length was set to $X_i = 1$ ($x_i = 30$ cm) and the downstream length was chosen to be $X_e = 5/3$ ($x_e = 50$ cm). This value for the downstream length was selected after establishing the fact that a longer length will not affect the results in the neighborhood of the recirculation region behind the step. The height of the calculation domain was selected so that the location $y + s = H = 10$ cm was sufficiently far away from the boundary layer. However, owing to some temperature stratification in the air tunnel, the freestream temperature, in the experiment, was not constant along the length of the plate, because the air in the freestream was confined in the test section of the tunnel and was heated slightly by the adjacent heated air layer, causing its temperature to increase along the length of the plate. This should be expected because the experimental apparatus is not an infinite domain as theoretically assumed in natural convection analysis. The small stable stratification in the freestream did not affect other freestream conditions significantly, and was taken into consideration while simulating the experiment. The freestream temperature varied almost linearly with $x^* = x + x_i$, and the measured values were used in the numerical simulation. In the present experimental study, the effect of three temperature differences $\Delta T = T_w - T_0 = 6.5$, 13.3, and 23°C ($Gr_{xi} = 2.512 \times 10^7$, 5.077×10^7, and 8.851×10^7) was examined. The corresponding axial variations of the freestream temperature were $T_\infty = 0.02584x^* + 24.6$, $T_\infty = 0.04797x^* + 25.4$, and $T_\infty = 0.07189x^* + 24.9$, respectively, where T_∞ is in degrees Celsius and x^* is in centimeters. A nonuniform grid system was adopted and a grid density of $Nx \times Ny = 120 \times 70$ was found to be sufficient in providing a grid-independent solution. For two mesh sizes of 120×70 and 160×100, the maximum changes in the predicted velocity, Nusselt number, and reattachment length were less than 3, 1.5, and 1%, respectively. Grid points were distributed such that they were tightly packed near the walls and location of the reattachment point where steep variations of velocities were expected. The grid system was varied smoothly in both the streamwise and transverse directions, forming the minimum and maximum dimensionless grid sizes of 0.0006 and 0.04 in the X direction, and 0.001 and 0.01 in the Y direction. A numerical solution was considered as converged when the maximum of the sum of each residuals of mass, momentum, and energy was less than 2×10^{-6}. All computations were performed on an HP 730 workstation, and it took about 1500 iterations in most cases to reach a converged solution.

Results and Discussion

The boundary-layer flow development as well as its two-dimensional nature was verified through flow visualizations and measurements of velocity and temperature across the width of the air tunnel, at various heights above the test surface. These measurements displayed a wide region (about 80% of the width of the heated test surface) around the center of the tunnel's width, where the flow velocity was almost constant (to within 5%) at a fixed height above the heated test surface, justifying the two-dimensional flow approximation. All reported streamwise velocity and temperature distributions in the transverse y direction were taken along the midplane ($z = 0$) of the plate's width, and only after the system had reached steady-state conditions.

Measurements of air velocity distributions were carried out in both regions upstream and downstream of the step. On the other hand, measurements of air temperature distributions were carried out only in the region downstream of the step because of limitations in the cold-wire setup. Figure 2 shows the measured and predicted dimensionless streamwise velocity distributions in both regions upstream ($X = -0.050$ and -0.083) and downstream ($X = 0.050$, 0.100, 0.200, 0.333, and 0.867) of the step for the case of $s = 16$ mm and $\Delta T = 23$°C ($Gr_{xi} = 8.851 \times 10^7$). Note that throughout this article the different

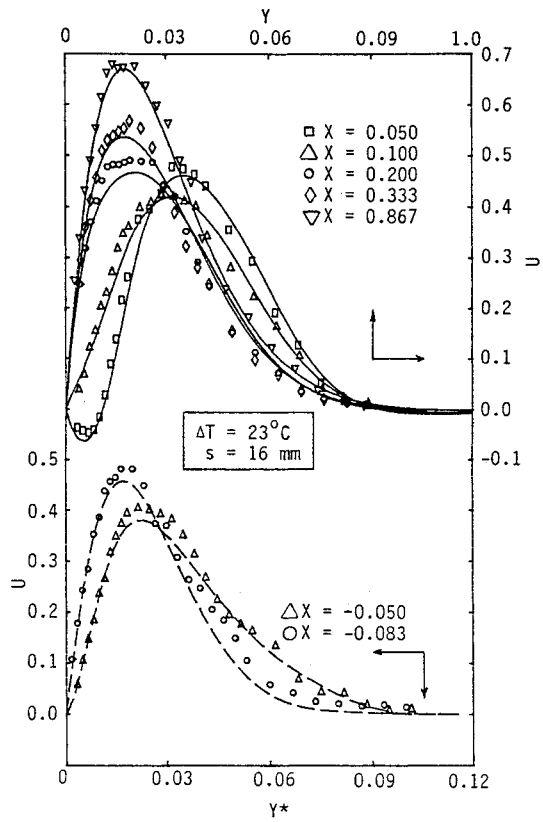

Fig. 2 Dimensionless streamwise velocity distribution.

symbols and different lines represent the measured and predicted results, respectively. As seen from Fig. 2, good agreement exists between the measured and predicted results (within 6%). The uncertainty in the measured U is ± 0.014 and in Y and Y^* is ± 0.007. In the region downstream of the step, the velocity distribution at $X = 0.050$ exhibits some negative velocity component, indicating that this distribution is located in the recirculation region that develops downstream of the step (as shown schematically in Fig. 1). Owing to the existence of this recirculation region, the location of the maximum velocity at this downstream location is at a longer distance from the heated plate than the rest of the distributions ($X = 0.100$, 0.200, 0.333, and 0.867). The figure also shows that outside this recirculation region (i.e., downstream of the reattachment point) the magnitude of the maximum velocity increases with increasing streamwise distance as a result of the downstream flow development. The figure clearly shows that the two velocity distributions upstream of the step ($X = -0.050$ and -0.083) do not exhibit any negative velocities, indicating that both of these velocity distributions are located outside (i.e., upstream) of the tiny recirculation region that develops in front, or upstream, of the step (as shown schematically in Fig. 1). Note that for the conditions in this experimental study, the length of the recirculation region that develops in front of the forward-facing step x_s was very small. The largest value of x_s was 1 cm (i.e., $X_s = 0.033$) for the conditions given in Fig. 2. Owing to the existence of the recirculation region upstream of the step, the magnitude of the maximum velocity decreases as the streamwise location approaches the step.

The effect of step height on the streamwise velocity distributions in the regions upstream and downstream of the step are illustrated in Figs. 3a and 3b, respectively, for various step heights at a temperature difference of $\Delta T = 13.3$°C ($Gr_{xi} = 5.077 \times 10^7$). In the region upstream of the step ($X = -0.050$ and -0.083 in Fig. 3a), the velocity distributions exhibit positive gradient at the wall, indicating that these locations are outside (upstream) the tiny recirculation region that develops

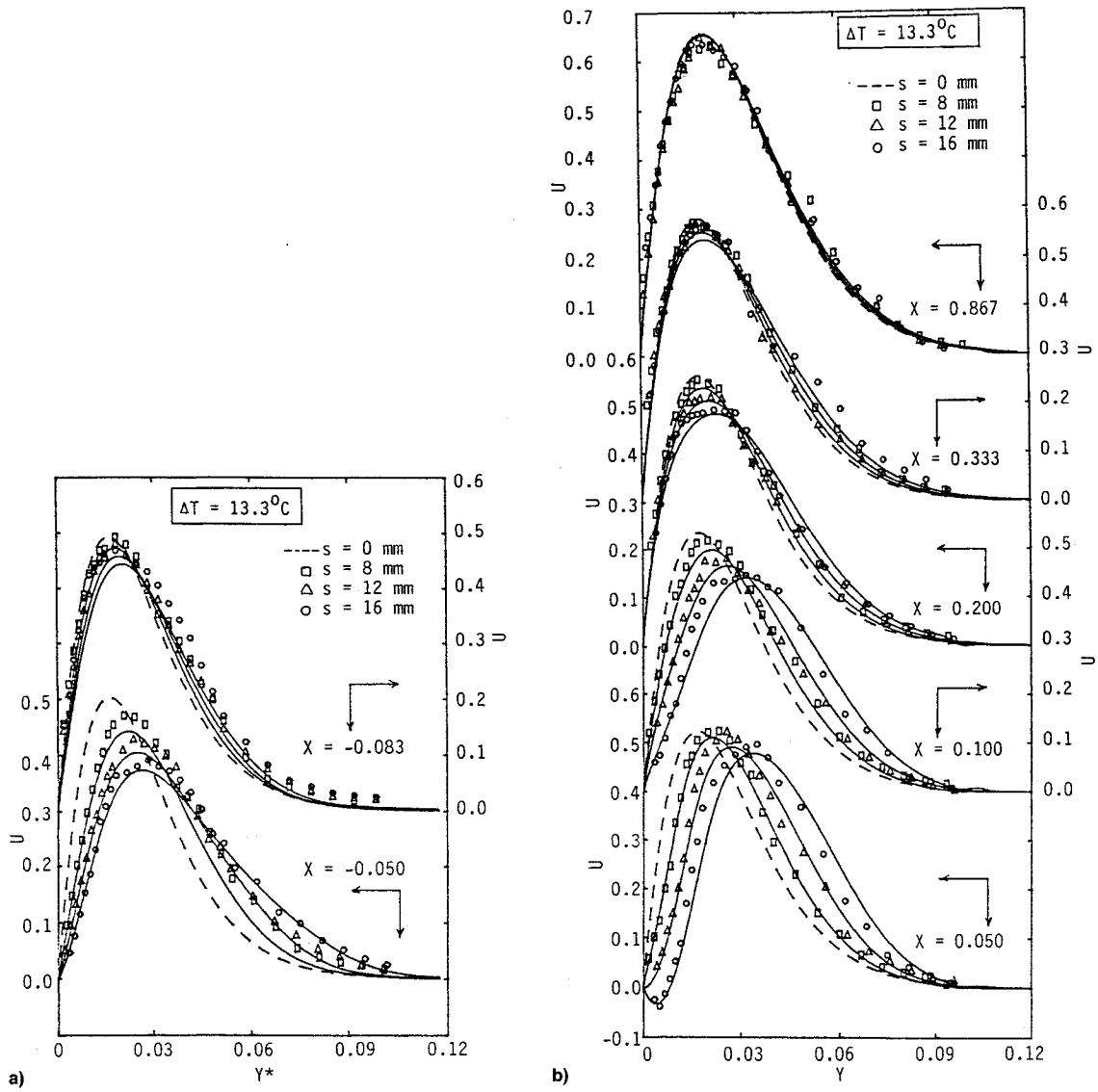

Fig. 3 Effect of step height on the velocity distribution a) upstream and b) downstream of the step.

in front (or upstream) of the step. As the step height decreases, the magnitude of the maximum velocity increases, with its location moving closer to the heated wall, and the velocity gradient at the heated wall increases (i.e., the wall shear stress increases). Figure 3a also shows that the effect of the step height on the velocity distributions upstream of the step diminishes as the distance increases from upstream of the step. Next, referring to the velocity distributions in the region downstream of the step in Fig. 3b, one can see that for the case of s = 16 mm, the velocity distribution at X = 0.050 exhibits a negative gradient at the wall, indicating that this location is inside the recirculation region that develops downstream of the step. For the other two step heights (s = 8 and 12 mm), the velocity distributions exhibit positive gradient at the wall, indicating that the location X = 0.050 is either downstream of the reattachment point and outside the recirculation region, for the conditions presented in the figure, or the recirculation region does not develop for these conditions.

From computations and flow visualization, it was determined that for the conditions shown in Fig. 3b a recirculation region downstream of the step does not develop for the step height s = 8 mm, but a recirculation region downstream of the step develops for the step heights s = 12 and 16 cm, with a reattachment length of 0.046 (corresponding to x = 1.4 cm, which is shorter than X = 0.050 or x = 1.5 cm, where the velocity distribution was measured and presented as in Fig. 3b) for s = 12 cm and 0.073 (corresponding to x = 2.2 cm) for s = 16 cm. Note that it was determined that a recirculation region starts to develop downstream of the step when the ratio of the boundary-layer thickness at the step to the step height δ_s/s is less than 1.7. The results in Fig. 3b illustrate that in the downstream region near the step (X = 0.050, 0.100, 0.200, and 0.333), as the step height decreases, the magnitude of the maximum velocity increases, while its location occurs closer to the heated wall as a result of change in the reattachment length (i.e., the size of the recirculation region); i.e., a smaller step height is associated with a smaller reattachment length. Figure 3b also shows that the effect of the step height on the velocity distributions downstream of the step decreases as the downstream distance from the step increases. This is because downstream of the reattachment point, the boundary layer redevelops and the shape of the velocity distributions (i.e., at X = 0.867) becomes similar to that of the flat plate (s = 0 mm), as shown in the figure.

Figures 4a and 4b illustrate the effect of buoyancy force induced by wall heating (ΔT = 6.5, 13.3, and 23°C corresponding to Gr_{xi} = 2.512 × 10^7, 5.077 × 10^7, and 8.851 × 10^7) on the velocity distributions upstream and downstream of the step, respectively, for the case of s = 16 mm. Figure 4a (for the region upstream of the step) clearly shows that as the buoyancy force increases (i.e., ΔT increases), both the velocity gradient at the heated wall (i.e., the wall shear stress) and the magnitude

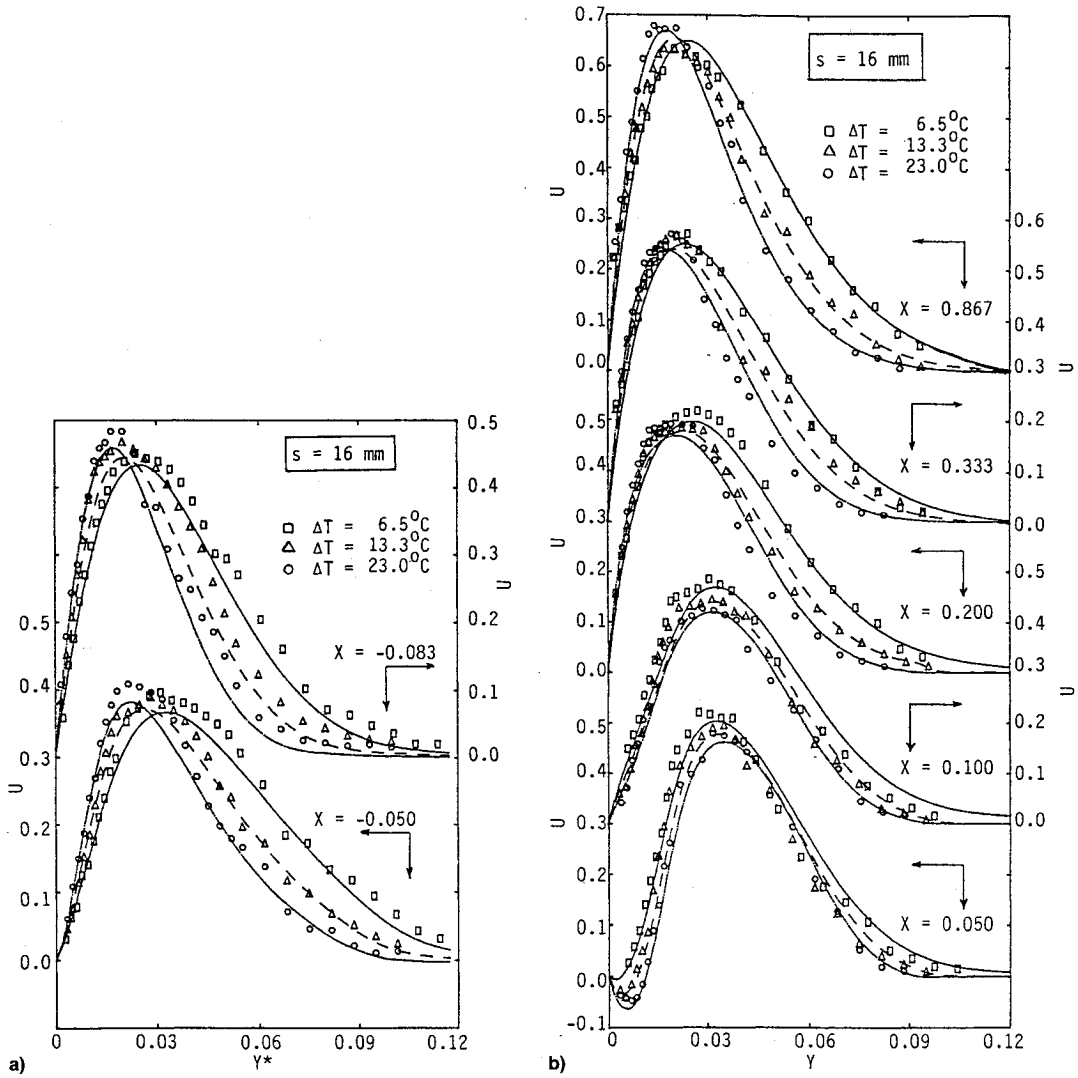

Fig. 4 Effect of buoyancy force on the velocity distribution a) upstream and b) downstream of the step.

of the maximum velocity increase, with the location of the maximum velocity getting closer to the heated wall and an accompanied decrease in the momentum boundary-layer thickness. In the region downstream of the step (Fig. 4b), the momentum boundary-layer thickness also decreases as the temperature difference increases. In the downstream region near the step (X = 0.050 and 0.100), with increasing buoyancy force, the velocity gradient at the heated wall (i.e., the wall shear stress) decreases. But this trend reverses farther downstream (X = 0.200, 0.333, and 0.867). From the flow visualization part of the study, it was determined that x_r (the size of the recirculation region that develops downstream of the step) increases as the buoyancy force increases (i.e., as the ΔT increases), because of the change in the magnitude of the maximum velocity approaching the step; i.e., a higher temperature difference is associated with a higher maximum velocity, as shown in Fig. 4a. For the step height of 16 mm, the ΔT of 6.5, 13.3, and 23°C resulted in x_r of 1.7, 2.2, and 2.5 cm, respectively. Note that the reattachment length increases linearly with buoyancy force Gr_{xi} (i.e., increasing ΔT), and it can be predicted to within 6% for the temperature difference range used in this experiment by the following correlation:

$$x_r = 1.227 \times 10^{-8} Gr_{xi} + 1.46 \qquad (11)$$

where x_r is in centimeters. In comparison with the mixed convection flow study of Abu-Mulaweh et al.,[2] the reattachment length in the natural convection flow is smaller than that of the mixed convection flow case.

The effect of step height (s = 16, 12, 8, and 0 mm) on the dimensionless temperature distributions $(T - T_\infty)/(T_w - T_\infty)$ for ΔT = 23°C ($Gr_{xi} = 8.851 \times 10^7$), at five different locations (X = 0.050, 0.100, 0.200, 0.333, and 0.867) downstream of the step, is illustrated in Fig. 5. As mentioned earlier, the freestream temperature was not constant in the experiment and varied almost linearly with x^*. Thus, the temperature was nondimensionalized with respect to the local freestream temperature. As can be seen from the figure, the measurements agree favorably with predictions within 8%. The uncertainty of the measured $(T - T_\infty)/(T_w - T_\infty)$ is ±0.025. In the neighborhood downstream of the step (X = 0.050 and 0.100), the figure shows that as the step height increases, the thermal boundary-layer thickness increases, and the temperature gradient at the heated wall decreases. This is because of the fact that a larger step height is associated with a larger reattachment length (i.e., larger recirculation region downstream of the step). The figure also shows that, similar to the downstream velocity distributions (Fig. 3b), the effect of step height on the temperature distributions diminishes slowly along the distance downstream (X = 0.200, 0.333, and 0.867), reaching a distribution of the flat plate (s = 0 mm) at X = 0.867.

The effect of buoyancy force, induced by wall heating (for ΔT = 6.5, 13.3, and 23°C corresponding to $Gr_{xi} = 2.512 \times 10^7$, 5.077×10^7, and 8.851×10^7), on the dimensionless downstream temperature distributions for the case of s = 16 mm is illustrated in Fig. 6 for five different downstream locations (X = 0.050, 0.100, 0.200, 0.333, and 0.867). The figure clearly shows that at all downstream locations the thermal

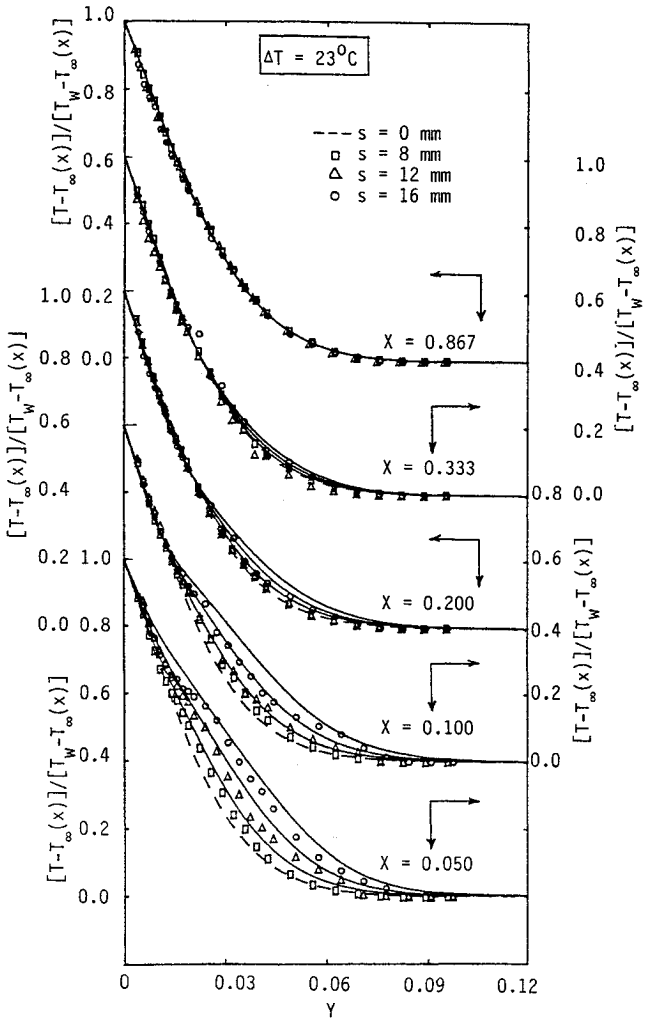

Fig. 5 Effect of step height on the temperature distribution.

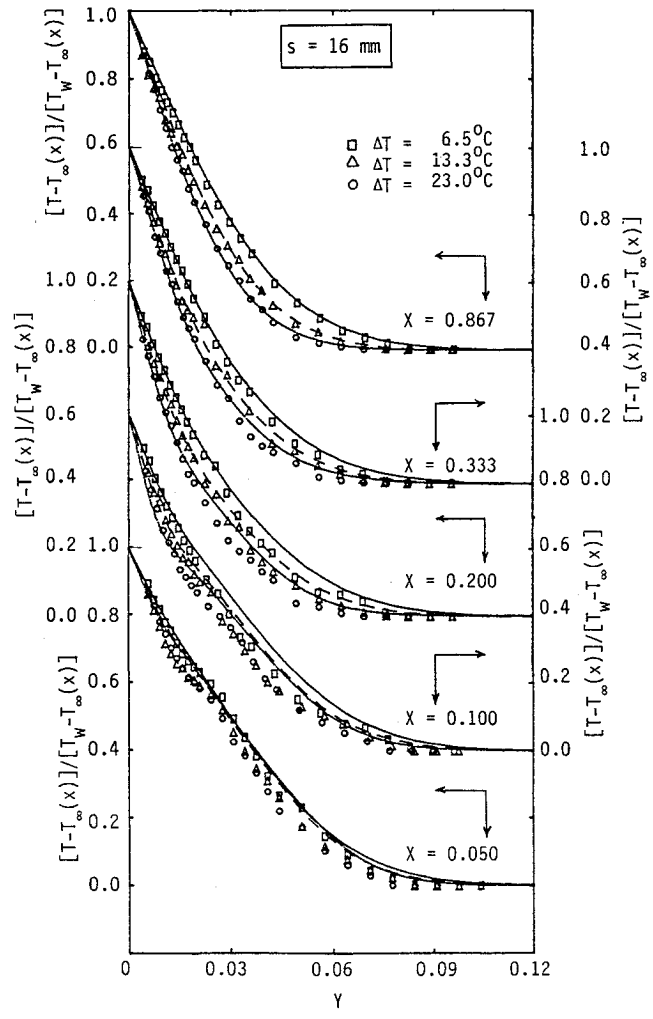

Fig. 6 Effect of buoyancy force on the temperature distribution.

boundary-layer thickness decreases and the temperature gradient at the heated wall increases (i.e., the heat transfer rate increases) as the temperature difference increases.

Figure 7 illustrates the effect of step height (for s = 8, 12, and 16 mm) on the axial variation of the local Nusselt number downstream of the step for the case of ΔT = 23°C (Gr_{xi} = 8.851 × 10^7). For comparison, the local Nusselt number for the flat plate (s = 0 mm) is also shown. For a given temperature difference and a step height, the local Nusselt number decreases rapidly from a maximum value at the step (X = 0) with increasing distance from the step, attains a minimum value to form a sharp valley, then increases rapidly to form a maximum peak value at some distance downstream, and finally decreases to approach asymptotically the flat plate value as the distance continues to increase in the streamwise direction. This behavior is attributed to the flow separation at the upper corner of the forward-facing step and the subsequent reattachment of the flow downstream.

Note in Fig. 7 that as the step height increases, the valley gets deeper, and the peak becomes higher. This is because larger steps cause a longer separation region. The figure also shows that for the cases where a recirculation region develops downstream of the step (s = 12 and 16 mm) the local Nusselt number attains lower values than that of the flat plate near the step, but downstream of the reattachment point the local Nusselt number is higher than that of the flat plate before it approaches the latter value. This is because the existence of an essentially stagnant fluid layer in the recirculation region causes a decrease in the heat transfer rate in that region, where as a strong mixing between cool and heated air that takes place

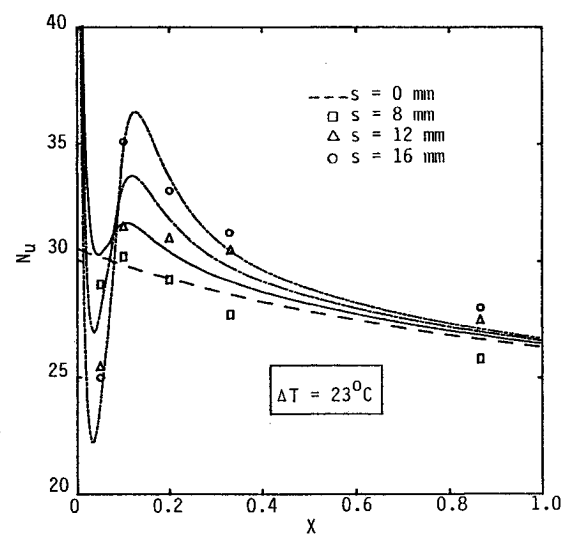

Fig. 7 Effect of step height on the axial variation of the local Nusselt number.

in the neighborhood of the reattachment region causes the wall heat transfer rate to increase. On the other hand, for the case where a recirculation region does not exist downstream of the step (s = 8 mm), the predicted local Nusselt number is higher than that of the flat plate for the conditions in the figure. This is because of the fact that in the absence of a recirculation

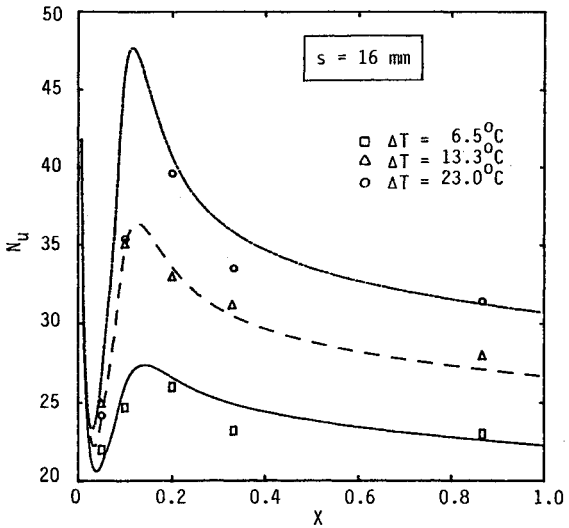

Fig. 8 Effect of buoyancy force on the axial variation of the local Nusselt number.

region on the downstream plate, a boundary layer develops from the upper corner of the step, which provides a larger heat transfer coefficient than that of a flat plate whose leading edge starts from the upstream plate. As can be seen from the figure, the results deduced from measurements agree favorably well with the predictions within 14%. The uncertainty in the measured X is ± 0.008 and in the Nu it is ± 0.75.

Figure 8 shows the effect of temperature difference (ΔT = 6.5, 13.3, and 23°C corresponding to $Gr_{xi} = 2.512 \times 10^7$, 5.077×10^7, and 8.851×10^7, respectively) on the axial variation of the local Nusselt number downstream of the step for the case of s = 16 mm. The figure clearly shows that the local Nusselt number is higher for a higher temperature difference. Both the valley and the peak of the Nusselt number get steeper with increasing temperature difference.

Conclusions

Measurements and predictions of laminar natural convection flow over a vertical two-dimensional forward-facing step reveal that the step height significantly affects the flow and thermal characteristics in the neighborhood downstream of the step, but this effect diminishes further downstream and the flow eventually approaches that of natural convection along a vertical flat plate. It has been found that downstream of the step the local Nusselt number forms a valley near the step and a peak downstream of the reattachment point before it assumes the flat plate value farther downstream. The valley gets deeper as the step height increases and the temperature difference decreases while the peak gets higher as both the step height and the temperature difference increase. The local Nusselt number downstream of the step increases with increasing temperature difference. Also the reattachment length increases as both the step height and the buoyancy force (i.e., the wall heating) increase. The measured results agree favorably with the numerical predictions.

Acknowledgments

This study was supported by a Grant from the National Science Foundation, NSF CTS-9304485. Bin Hong assisted in the numerical computations.

References

[1]Abu-Mulaweh, H. I., Armaly, B. F., and Chen, T. S., "Measurements of Laminar Mixed Convection Flow over a Horizontal Forward-Facing Step," *Journal of Thermophysics and Heat Transfer*, Vol. 7, No. 4, 1993, pp. 569–573.

[2]Abu-Mulaweh, H. I., Armaly, B. F., Chen, T. S., and Hong, B., "Mixed Convection Adjacent to a Vertical Forward-Facing Step," *Proceedings of the 10th International Heat Transfer Conference* (Brighton, England, UK), edited by G. F. Hewitt, Vol. 5, Taylor and Francis, Washington, DC, 1994, pp. 423–428.

[3]Abu-Mulaweh, H. I., Armaly, B. F., and Chen, T. S., "Measurements in Buoyancy-Opposing Laminar Flow over a Vertical Forward-Facing Step," *International Journal of Heat and Mass Transfer* (to be published).

[4]Baron, A., Tsou, F. K., and Aung, W., "Flow Field and Heat Transfer Associated with Laminar Flow over a Forward-Facing Step," *Proceedings of the 8th International Heat Transfer Conference*, Vol. 3, Hemisphere, Washington, DC, 1986, pp. 1077–1082.

[5]Keyhani, M., Prasad, V., and Cox, R., "An Experimental Study of Natural Convection in a Vertical Cavity with Discrete Heat Sources," *24th National Heat Transfer Conf.*, American Society of Mechanical Engineers, New York, 1987 (Paper 87-HT-76).

[6]Shakerin, S., Bohn, M., and Loehrke, R. I., "Natural Convection in an Enclosure with Discrete Roughness Elements on a Vertical Heated Wall," *International Journal of Heat and Mass Transfer*, Vol. 31, No. 7, 1988, pp. 1423–1430.

[7]Hung, Y. H., and Shiau, W. M., "Local Steady-State Natural Convection Heat Transfer in Vertical Parallel Plates with a Two-Dimensional Rectangular Rib," *International Journal of Heat and Mass Transfer*, Vol. 31, No. 6, 1988, pp. 1279–1288.

[8]Joshi, Y., Wilson, T., and Hazard, S. J., III, "An Experimental Study of Natural Convection from an Array of Heated Protrusions on a Vertical Surface in Water," *Journal of Electronic Packaging*, Vol. 111, No. 1, 1989, pp. 121–128.

[9]Lin, T. Y., and Hsieh, S. S., "Natural Convection of Opposing/Assisting Flows in Vertical Channels with Asymmetrically Discrete Heated Ribs," *International Journal of Heat and Mass Transfer*, Vol. 33, No. 10, 1990, pp. 2295–2309.

[10]Burak, V. S., Volkov, S. V., Martynenko, O. G., Khramtsov, P. P., and Shikh, I. A., "Experimental Study of Free Convection Flow on a Vertical Plate with a Constant Heat Flux in the Presence of One or More Steps," *International Journal of Heat and Mass Transfer*, Vol. 38, No. 1, 1994, pp. 147–154.

[11]Ramachandran, N., Armaly, B. F., and Chen, T. S., "Measurements and Predictions of Laminar Mixed Convection Flows Adjacent to a Vertical Surface," *Journal of Heat Transfer*, Vol. 107, No. 3, 1985, pp. 636–641.

[12]Abu-Mulaweh, H. I., Armaly, B. F., and Chen, T. S., "Laminar Natural Convection Flow over a Vertical Backward-Facing Step," *Journal of Heat Transfer*, Vol. 117, No. 4, 1995, pp. 895–901.

[13]Patankar, S. V., *Numerical Heat Transfer and Fluid Flow*, Hemisphere, Washington, DC, 1980.